Pertanika J. Sci. & Technol. 24 (2): 451 - 463 (2016)

PERTANIKA JOURNALS

SCIENCE & TECHNOLOGY

Journal homepage: http://www.pertanika.upm.edu.my/

CFD Investigation of Transonic Axial Compressor Rotor Blade at Various Off-Design Conditions

Pauline Epsipha*, Mohammad, Z. and Kamarul, A. A.

Department of Aerospace Engineering, Engineering Faculty, Universiti Putra Malaysia, Selangor, 43400, Selangor, Malaysia

ABSTRACT

Flow separation over blade surfaces is an important parameter and its reduction or elimination can improve better aerodynamic performance, efficiency and stall margin. In this work, numerical investigation has been carried out to study the flow separation and performance analysis of a transonic axial compressor rotor blade at off-design operating conditions. The off-design cases studied comprised of compressor operation at 80%, 90%, 100% and 105% on the on-design rotational speed. The results are validated with experimental work from literature. Additionally, 3D flow visualisations and performance parameters were examined in detail to understand the blade to blade relative mach number distributions and shock front created by the model. Finally, the benefits of unsteady simulation on axial compressor blade performance predictions were examined.

Keywords: Compressor rotor blade, Numerical investigation, Flow separation, Off-design cases, Shock front, Efficiency

INTRODUCTION

In recent years, in the field of turbo machinery and aero-engine, transonic axial flow compressors have played important role to attain higher pressure ratios which help in increasing the efficiency and reducing the size and weight of the engine. The increase in pressure ratio at every single stage of compressor counts the reciprocating results on operational and fuel cost. Thus, progress in the performance chart of the compressors plays a crucial part in research as well engine manufacturing.

The flow field which progresses inside a transonic axial compressor is particularly complicated and puts forth huge challenges on compressor designers. Critical flow challenges such as secondary flows, shock waves, shock/

Article history:
Received: 17 February 2016
Accepted: 22 April 2016

E-mail addresses:
paul.totty89@gmail.com (Pauline Epsipha),
mzuber@upm.edu.my (Mohammad, Z.),
aekamarul@upm.edu.my (Kamarul, A. A.)
*Corresponding Author

ISSN: 0128-7680

boundary layer interactions, and flow separation over the blade surfaces decrease the efficiency and encourage energy losses (Cumpsty, 1989; Law & Wadia, 1993; Denton & Xu, 1998).

Various experimental and numerical investigations of transonic compressors have been carried out since 1960 (Chen et al., 1991; Freeman & A., 1992). As transonic compressors paved the way for investigation over supersonic compressors, various researches of its kind have been conducted over the past decades. A significant number of researches were carried out for new development in design (Reid & Moore, 1978; Strazisar, 1985), which in turn gave a wider perspective over the loss mechanisms (Strazisar, 1985; Hah & Reid, 1991). These deeper understanding later emerged as concepts for active and passive techniques to decrease the loss (Cumpsty, 1989; Denton & Xu, 1998; Calvert et al., 2003) and increase the efficiency and stall margin.

According to Biollo (Biollo & Benini, 2013), in transonic axial flow compressors, the typical value achieved for the rotor inlet relative flow at the tip is Mach = 1.3. And the total pressure ratio achieved for high efficiency transonic axial flow compressors (civil aviation) is in the order of 1.7-1.8 along with the tip speed of 450 m/s and high stage loading in the order of 1.0. Despite a decade of research on it, the concept of further performance enhancement in transonic compressor is still under investigation.

The primary goal of this research is to investigate the flows within the transonic axial flow compressor rotor blade across a wide range of off-design operating conditions. The off-design cases studied comprised compressor operation at 80%, 90%, 100% and 105% at on-design rotational speed. The opportunity to study the flow separation and performance of rotor blade would provide a broad understanding of its reduction/elimination capacity and thereby improve efficiency and stall margin.

NASA ROTOR 37

The NASA rotor 37 is an isolated low aspect ratio inlet rotor for an axial core compressor. This rotor is a transonic compressor with a tip speed of 454 m/s and produces a relatively high pressure ratio of 2.1 (Denton, 1997). This 'blind' test case study is widely used in many research programmes, which intends to study the flow and aerodynamic parameters at transonic speed level. Initially, it was designed and tested at NASA lewis research centre without any inlet guide vanes for four related axial flow compressor stage. These stages were tested for a wide range of design parameters especially aspect ratio and pressure ratio by Reid and Moore (1978). A more detailed performance parameters of this rotor 37 were reported by Reid and Moore (1980, 1982). The rotor was again tested in a single-stage compressor facility at NASA Glenn by Suder (Kenneth & Celestina, 1996; Kenneth, 1997; Suder et al. 1995) and by various researchers. Table 1 shows the design parameters for the Rotor 37 and Figure 1 shows the meridional view of NASA Rotor 37 (Benini et al., 2011).

Table 1
Aerodynamic design parameters

Number of blades	37
Blade type	Multiple Circular Arc
Rotational Speed	17188.7 rpm
Inlet hub-tip diameter ratio	0.7
Blade aspect ratio	1.19
Tip solidity	1.29
Tip clearance	0.0356 cm (0.45% of blade span)
Tip speed	454 m/s
Adiabatic efficiency	0.877
Design pressure ratio	2.106
Design mass flow rate	20.19 kg/s
Choked mass flow rate	20.93 kg/s

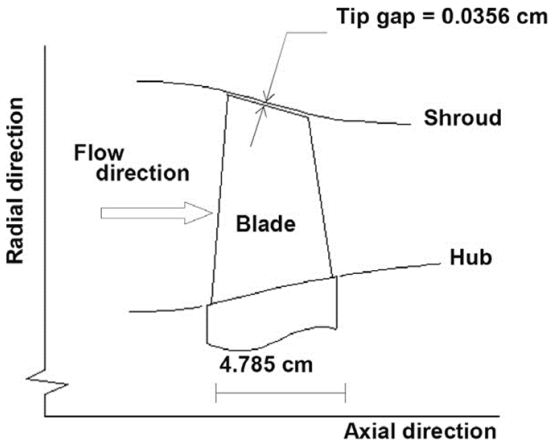

Figure 1. Meridional view of NASA Rotor 37 (Benini et al., 2011)

TURBULENCE THEORY

Navier–Stokes equations

The Navier-Stokes equations describing the flow of compressible gases are a non-linear set of partial-differential equations (PDEs) governing the conservation of mass, momentum and energy of the gaseous motion.

The conservation of mass equation (Continuity Equation) in tensor notation can be formulated as:

$$\frac{\partial \rho}{\partial t} + \frac{\partial}{\partial x_i}\left(\rho\, u_i\right) = 0$$

where ρ and u_i are gas density and flow velocity respectively. In tensor notation, the momentum equation that represents the Navier-stokes equation is:

$$\frac{\partial}{\partial t}(\rho u_i) + \frac{\partial}{\partial x_j}(\rho u_i u_j + p\delta_{ij} - \tau_{ij}) = \rho f_i$$

where *P* and τ_{ij} are gas pressure and mean rate of stress tensor respectively and f_i is the acceleration of the gas due to body forces.

Reynolds-averaged Navier–Stokes (RANS) equations

The Reynolds-averaged Navier–Stokes (RANS) equations are the oldest form of time averaged equation for turbulence modelling. In turbulent flow, even in a steady state, all the variables tend to fluctuate with time. Reynolds (1895) introduced the idea that the turbulent flow total variable (U) can be expressed as the sum of the mean ($\bar{u}$) and fluctuating variable (u'). The $\bar{u}$ (overbar) represents the time averaged quantity as:

$$U(t) = \bar{u} + u'(t)$$

This decomposition equation can be substituted for all the variables in the flow (u, v, w, P, ρ). RANS describing the time-evolution of the mean flow quantities Ui and P can be written as:

$$\frac{\partial U_i}{\partial t} + Uj\frac{\partial U_i}{\partial x_j} + \frac{1}{\rho}\frac{\partial P}{\partial x_i} = \frac{1}{\rho}\frac{\partial}{\partial x_j}(\bar{\tau}_{ij} + \lambda_{ij})$$

where $\bar{\tau}_{ij}$ is fluid stress tensor which is evaluated in terms of the mean flow quantities and λ_{ij} is the Reynolds or turbulent stress tensor which is given as:

$$\lambda_{ij} = -\rho\overline{u'_\iota u'_\jmath}$$

Shear-Stress Transport model

Predicting the flow separation from a smooth surface is considered as one of the main issues in turbulence modelling. Standard two equations do not have the capability to predict the amount of flow separation under adverse pressure gradient conditions. Hence, several advanced turbulence models were developed for this application. One such model is known as Shear Stress Transport (SST) turbulence model, which is a combination of k-ε and k-ω models.

The turbulence model used in this computation is k-ω based Shear-Stress-Transport (SST) model which was designed to give a highly accurate prediction of the onset and the amount of flow separation under adverse pressure gradients by the inclusion of transport effects into the formulation of the eddy-viscosity. This results in a major improvement in terms of flow separation predictions.

The turbulent eddy viscosity is computed from the turbulent kinetic energy and turbulent frequency as:

$$\mu_T = {}^{\rho k}/_{\omega}$$

METHODOLOGY

A steady state simulation was carried out for 80, 90, 100 and 105% design speed of the rotor 37 using ANSYS CFX and the resultant flow field was further investigated along with an overall performance map. The results obtained from the numerical analysis were compared with the experimental data for validation purposes. It should be noted that no stage approach has been carried out but only a rotor was used in the frozen approach.

Modelling and Mesh Generation

The data points for the rotor model and the computational domain were collected as a .curve and .inf (bladegen files), where it is interlinked to the ANSYS Turbo grid meshing tool. Figure 2 shows the 3D model of the rotor along with the flow domain in the entire compressor. The meshing of the domain with blade is made using ANSYS Turbo grid package. *y*+ value for the generated mesh near the wall zones are maintained at 2 which is as per the turbulence modelling requirements. Thus, the discretisation of the structured grid with around 1,800,000 cells was generated. A single passage simulation is modelled and numerically solved with an assumption that the flow is periodic within the passage. Figure 3 shows the picture of discretised rotor model with flow domain.

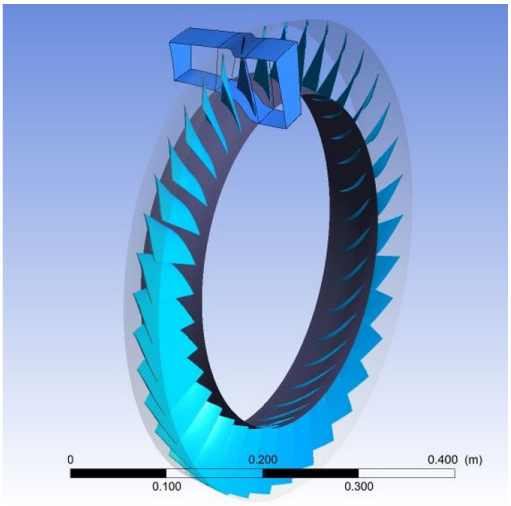

Figure 2. Rotor alone model

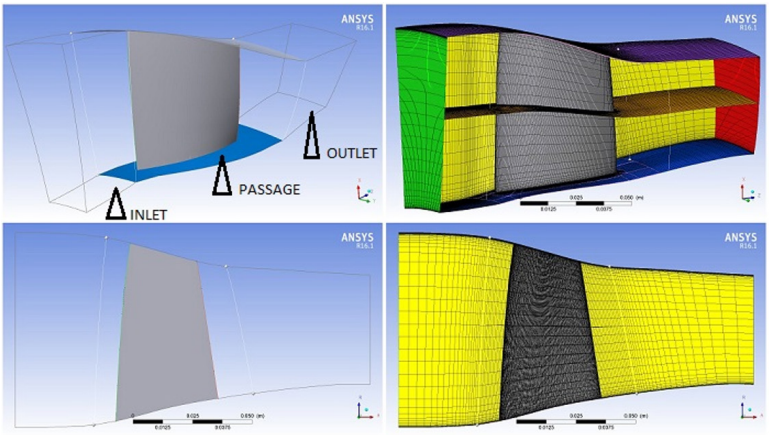

Figure 3. Meshed Rotor model

Flow Analysis

The flow analyses were carried out using a commercial CFD package. The ANSYS CFX executes 3D Reynolds-averaged Navier-stokes equations based on the finite volume numerical method. The flow fluid was assumed to be an Ideal gas, having constant specific heats. K-ω Shear Stress Transport (SST) turbulence model was equipped for the present study which is governed by adverse pressure gradients. This model is not able to capture the fine vortex micro structures development We neglect the necessity as it is not of primary concern. To confirm that results are independent of the mesh, grid dependency tests were carried out for Y+ values as 1, 2, 5 and total of around 1,800,000 cells were taken into account for the final domain.

The walls of the domain were assumed to be adiabatic and hydraulically smooth which is specified as no slip condition. It indicates that the fluid sticks to the wall and moves with the same velocity as the wall (if it is moving). For validation purposes, calculations were run at the design speed of the rotor (1800 rad/s). The boundary conditions of total pressure and total temperature were imposed at the inlet (P_{inlet} = 101330 Pa, T_{inlet} = 288.15 K) to recreate the experimental boundary conditions.

As an outlet condition, the static pressure was imposed as a mass-averaged value, in order to find the Design mass flow and choked mass flow condition at On-design speed. The turbulent intensity was fixed to a 5% value. The rotor was run at frozen rotor condition in order to make a smooth flow inside the domain. For every steady simulation, the convergence criteria (RMS residuals) was inflicted as 1 x 10^{-6}. Figure 4 shows the boundary conditions applied to the flow domain.

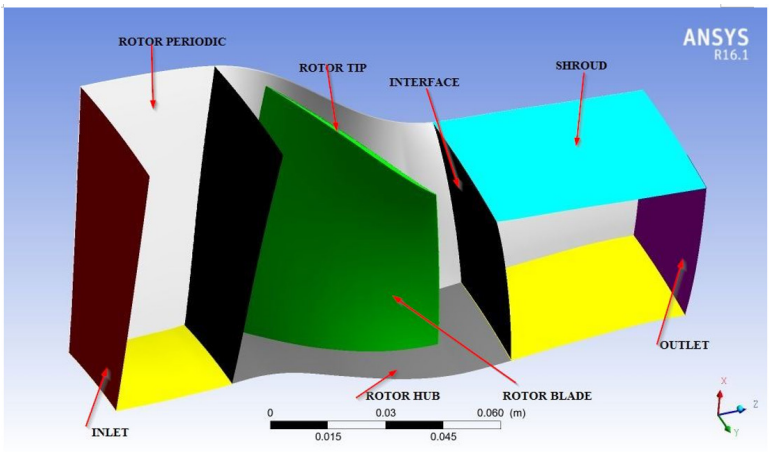

Figure 4. Flow domain boundary conditions.

Validation of Numerical Results

Validation processes were carried out upon the on-design rotor speed (1800 rad/s) and the numerical results were plotted against experimental results of baseline compressor performance extracted from Suder et al. (1995). The primary performance measure investigated is total pressure ratio which is ratio between exit pressure and inlet pressure. Figure 5 shows graph for total pressure ratio and adiabatic efficiency against the various mass flow rate condition. The percentage error calculated were 1.24% and 1.61%. Through the plotted graph, it is witnessed that computed results which are below than 5% are in good agreement with the experimental data at on-design speed.

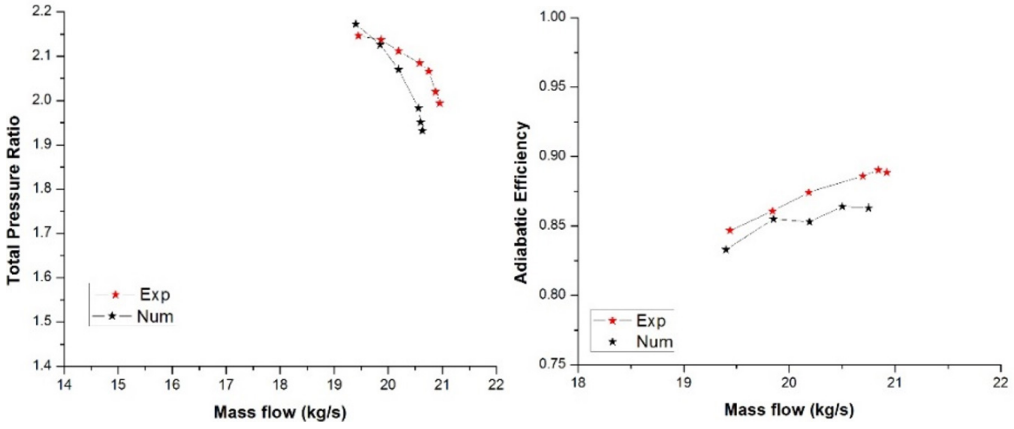

Figure 5. Performance characteristics of design speed (1800rad/s)

RESULTS AND DISCUSSION

The comparative performance map of the baseline compressor at on- design speed and off-design speed is shown in Figure 6. Total pressure ratio and adiabatic efficiency against the mass flow rate were plotted in the performance map below. The red plots indicate experimental case results while the black plots indicate the numerical case of the baseline rotor. As the on-design speed is validated properly with a percentage error of 1.24% and 1.61%, the off-design speed of 90% experimental values were ignored. It is monitored that among the off/on design conditions, the flow follows the consistent patterns and the highest efficiency occurred at on-design speed. The flow physics of the compressor rotor for different off-design conditions were studied using velocity vectors, mach number contours and velocity streamlines as mentioned below.

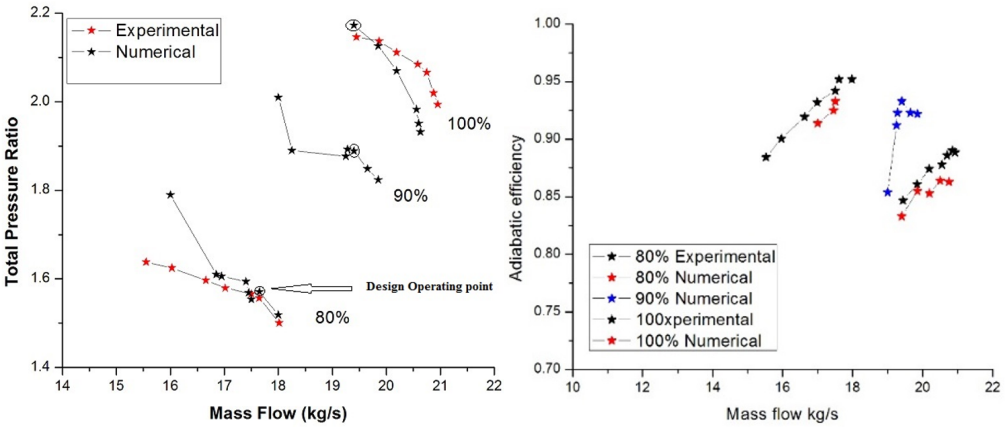

Figure 6. Overall Performance characteristics

Mach number

Figure 7 shows the comparative mach number contours computed along the on-design speed and varied off design conditions. Concerning the calculated flow field, the plots were computed at 70% span blade to blade mach number. It is observed that a strong shock front was created and flow separation was combined along the flow at the suction side of the rotor blade at 100% and 105% design speed. While in the 90%, the formation of shock and flow separation region was much weaker compared to previous flows.

In 80% design speed, the flow was much smoother and flow separation was almost unnoticed. With the help of a well captured model, the reduction in shock strength is seen to directly affect the pressure ratio reduction which disturbs the efficiency of the compressor rotor. It also indicates the fact that blade boundary layer and its interaction have been properly captured by the numerical simulation. Table 2 indicates the relative inlet mach number for each speed.

Table 2
Variation of Inlet Mach number for various speed

% speed	M_{rel} at hub	M_{rel} at tip
80	0.91	1.15
90	0.94	1.29
100	1.02	1.33
105	0.97	1.45

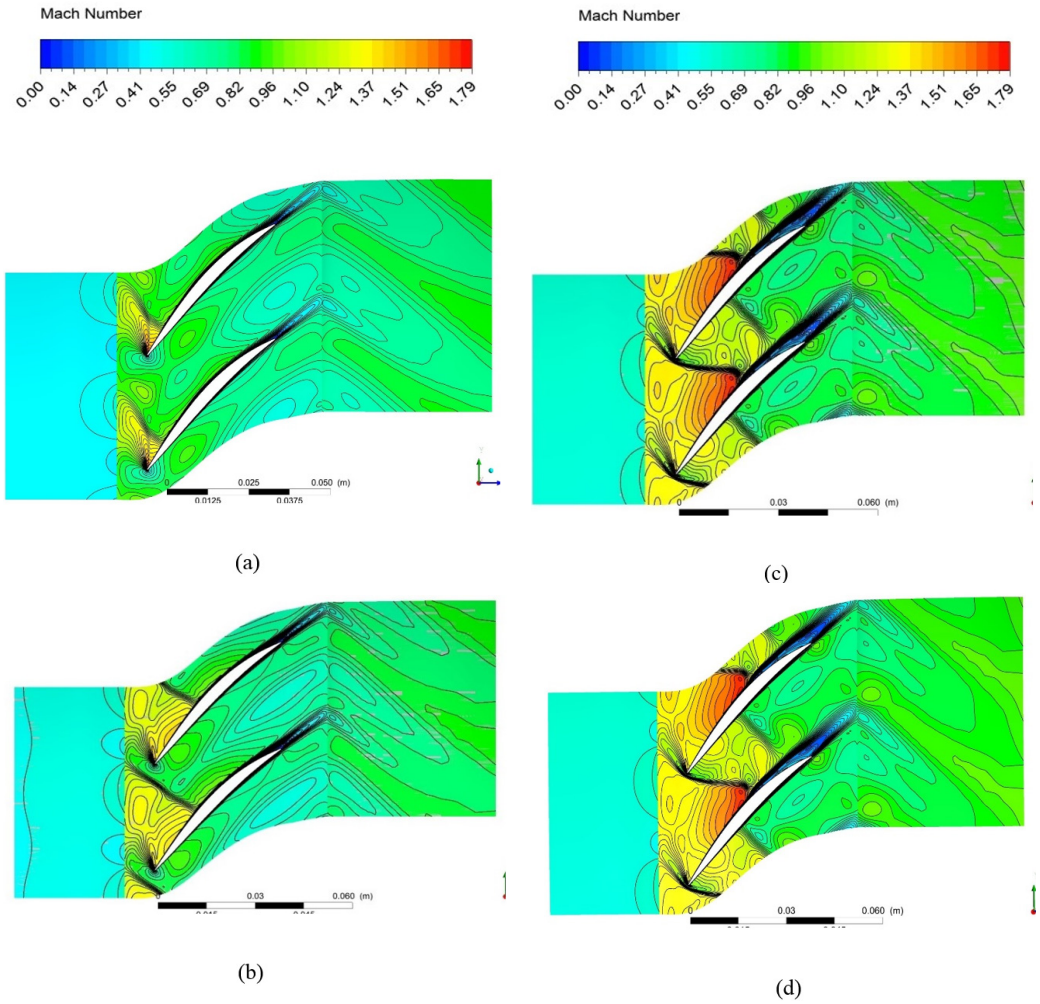

Figure 7. Comparative Mach number contours at 70% span at various off design conditions, (a) 80% (b) 90% (c) 100% (d) 105%

Velocity

Figure 8 displays the comparative velocity vector plots for peak efficiency condition at baseline rotor's on/off design compressor speed. Vector plots are plotted at the 95% span of blade to blade view for the velocity distribution over the different operating conditions. As shown in the contour, high velocity is observed at the inlet condition which produces shock front where

it gets reduced from the blade surface at trailing edge because of the flow separation. Though there is a difficulty to produce the well-defined tip clearance vortex pattern, its shock interaction with the flow is captured reasonably well.

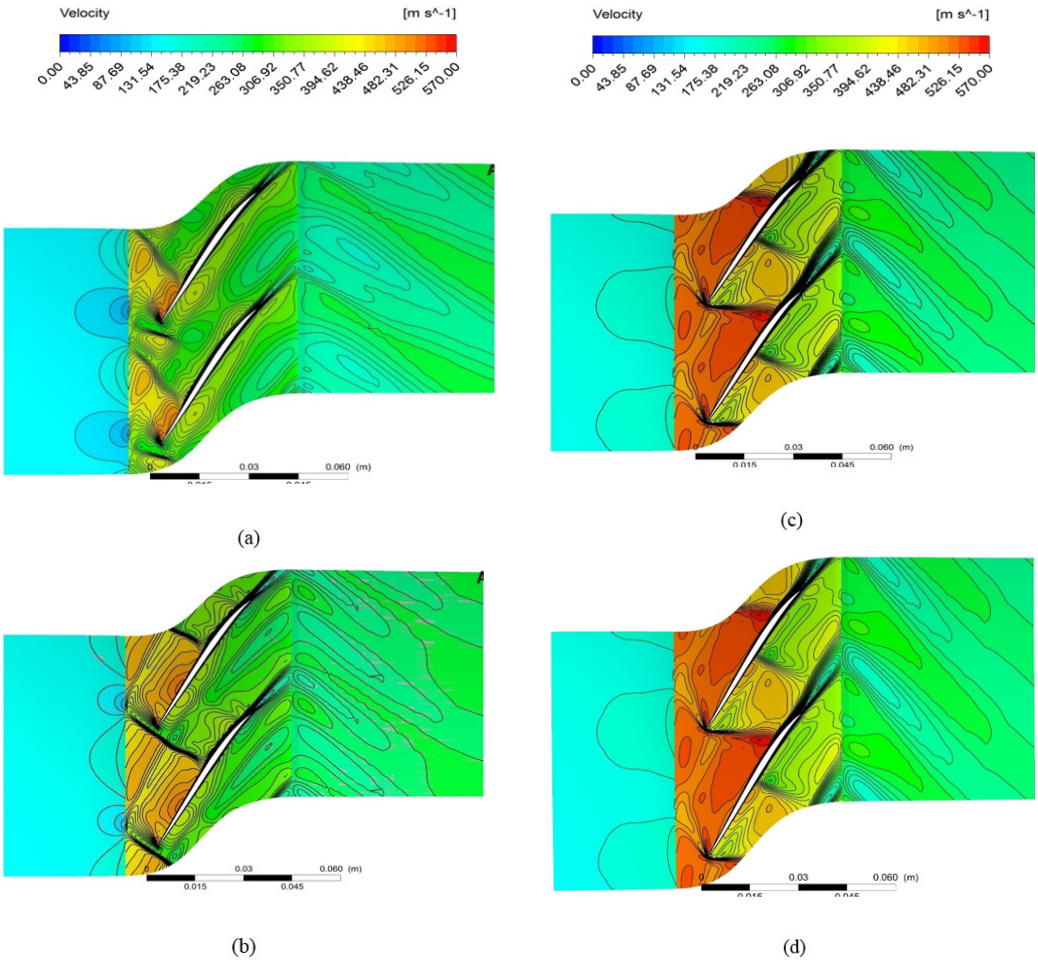

Figure 8. Comparative Velocity plot at 95% span at Various off design conditions, (a) 80% (b) 90% (c) 100% (d) 105%

Streamline

Figure 9 shows the comparative detailed streamline patterns in suction side of the rotor for various design speed at maximum efficiency condition. The streamlines discharged from the leading edge and the separation line are created at the suction side boundary. The 3D streamline patterns indicate fairly well the internal flow conditions created at suction of the rotor span. A form of flow disruption were created because of the shock and the flow separation near the trailing edge which were also captured in the blade to blade mach number contour as seen in Figure 7. Also for the off-design condition at maximum efficiency state, clearly reveals that there is less flow separation created compared with the on-design speed.

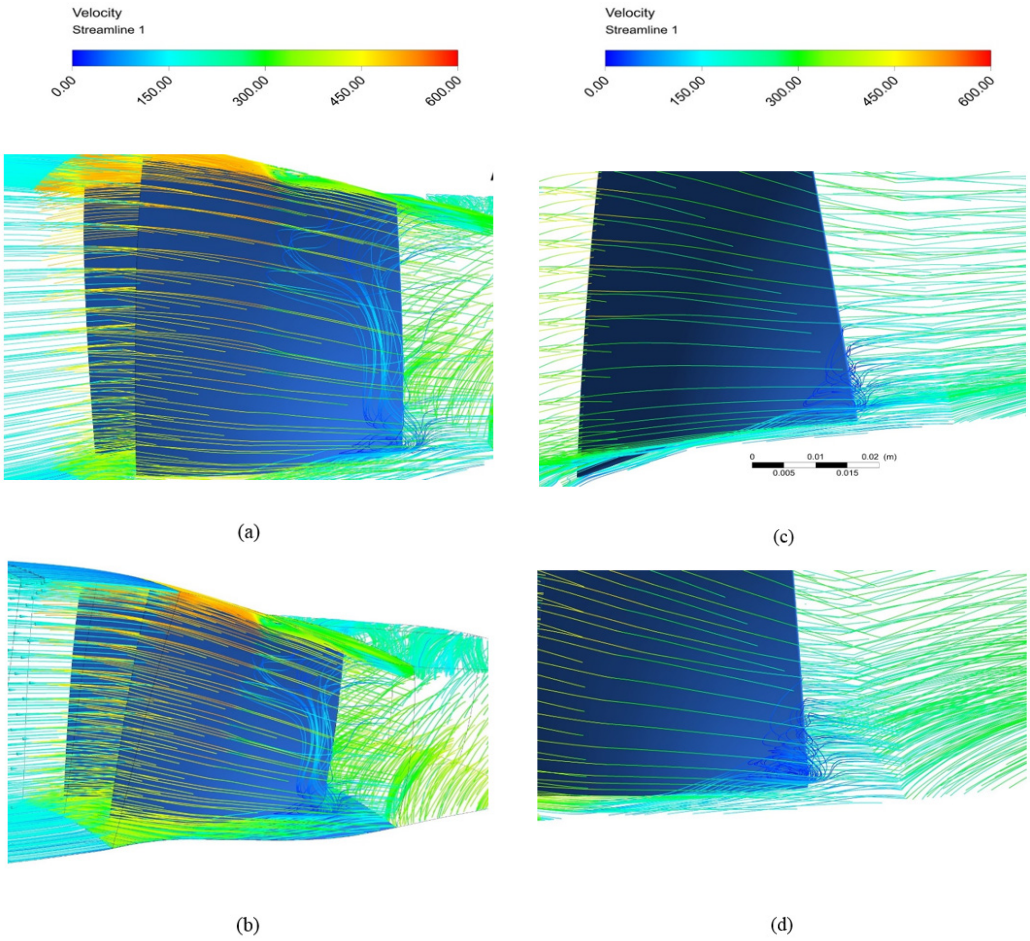

Figure 9. Comparative streamlines on the maximum efficiency rotor state at various off design conditions (a) 105% (b) 100% (c) 90% (d) 80%

CONCLUSION

A computational flow steady analysis for a transonic axial flow compressor rotor at on-design speed (1800 rad/s) and various off design conditions at 80%, 90% and 105% was carried out. The flow pattern analysis was conducted for the mach number distribution, velocity vector and streamline patterns to provide a detailed conclusion. The purpose of this paper was to study the flow and performance parameters for better understanding over the off-design condition. A weak flow separation condition was observed in mach number contour at the off design conditions at 80% and 90% compared with 100% and 105% design speed. It was found that the efficiency of the rotor has a direct impact from the shock front created. Thus, there is a reduction in efficiency due to the poorly produced shock front in 80% and 90% design speed along with a big pressure ratio difference. Even though the velocity condition at 105% design speed looks better than on-design speed (1800 rad/s), due to unstable flow condition along various mass flow rate, reduced efficiency was noted which negatively impacts the efficiency.

ACKNOWLEDGEMENTS

The first author would like to thank Universiti Putra Malaysia (UPM) for providing funds through the UPM GP –IPM/2014/9444000 grant.

REFERENCES

Benini, E., Biollo, R., & Ponza, R. (2011). Efficiency enhancement in transonic compressor rotor blades using synthetic jets: A numerical investigation. *Applied Energy*, *88*(3), 953–962. http://doi.org/10.1016/j.apenergy.2010.08.006

Biollo, R., & Benini, E. (2013). Recent advances in transonic axial compressor aerodynamics. *Progress in Aerospace Sciences*, *56*, 1–18. http://doi.org/10.1016/j.paerosci.2012.05.002

Calvert, W. J., Emmerson, P. R., & Moore, J. M. (2003). Design, Test and Analysis of a High-Pressure-Ratio Transonic Fan. In *Volume 6: Turbo Expo 2003, Parts A and B* (pp. 417–427). ASME. http://doi.org/10.1115/GT2003-38302

Chen, G. T., Greitzer, E. M., Tan, C. S., & Marble, F. E. (1991). Similarity Analysis of Compressor Tip Clearance Flow Structure. *Journal of Turbomachinery*, *113*(2), 260. http://doi.org/10.1115/1.2929098

Cumpsty, N. A. (1989). *Compressor aerodynamics*. *Compressor Aerodynamics*. Longman Scientific & Technical. Retrieved from http://www.amazon.com/Compressor-Aerodynamics-N-Cumpsty/dp/1575242478/ref=pd_sim_b_2

Denton, J. D. (1997). Lessons from rotor 37. *Journal of Thermal Science*, *6*(1), 1–13. http://doi.org/10.1007/s11630-997-0010-9

Denton, J. D., & Xu, L. (1998). The exploitation of three-dimensional flow in turbomachinery design. *Proceedings of the Institution of Mechanical Engineers -- Part C -- Journal of Mechanical Engineering Science*, *213*(2), 125–137. http://doi.org/10.1243/0954406991522220

Freeman, C., & A., C. N. (1992). Method for the prediction of supersonic compressor blade performance. *Journal of Propulsion and Power*, *8*(1), 199–208.

Hah, C., & Reid, L. (1991). A viscous flow study of shock-boundary layer interaction, radial transport, and wake development in a transonic compressor, *114*(July 1992). http://doi.org/10.1115/1.2929177

Law, C. H., & Wadia, A. R. (1993). Low Aspect Ratio Transonic Rotors: Part 1—Baseline Design and Performance. *Journal of Turbomachinery*, *115*(2), 218–225. http://doi.org/10.1115/1.2929226

Moore Royce, D., & Reid, L. (1982). Performance of Single stage Axial Transonic Compressor with rotor and stator as pect ratios of 1.19 and 1.26 Respectively and with design pressure ratio of 1.82. *Nasa Technical Paper*, (November 1978), 105. http://doi.org/NASA-TP-1338

Reid, L., & Moore, R. D. (1978). Design and overall performance of four highly loaded, high speed inlet stages for an advanced high-pressure-ratio core compressor. Retrieved from http://ntrs.nasa.gov/search.jsp?R=19780025165

Strazisar, a. J. (1985). Investigation of flow phenomena in a transonic fan rotor using laser anemometry. *Journal of Engineering for Gas Turbines and Power*, *107*(2), 427. http://doi.org/10.1115/1.3239743

Suder, K. L. (1997). Blockage Development in a Transonic, Axial Compressor Rotor. http://doi.org/10.1115/1.2841741

Suder, K. L., & Celestina, M. L. (1996). Experimental and Computational Investigation of the Tip Clearance Flow in a Transonic Axial Compressor Rotor. *J. Turbomach.*, *118*(2), 218–229. http://doi.org/10.1115/1.2836629

Suder, K. L., Chima, R. V., Strazisar, a. J., & Roberts, W. B. (1995). The Effect of Adding Roughness and Thickness to a Transonic Axial Compressor Rotor. *Journal of Turbomachinery*, *117*(4), 491. http://doi.org/10.1115/1.2836561